Spatio-temporal Correlations of Terrestrial Laser Scanning

Raumzeitliche Korrelationen beim terrestrischen Laserscanning

Stephanie Kauker, Christoph Holst, Volker Schwieger, Heiner Kuhlmann, Steffen Schön

This contribution investigates correlations in terrestrial laser scanning on the scientific level. It summarizes recent approaches to model correlations, to develop measurement scenarios for the determination of correlations as well as to identify the influence of the correlations on estimation procedures. It can be concluded that the following challenges are remaining: complete synthetic modelling as well as the development of appropriate measurement scenarios to determine correlations in an empirical way. Additionally, the research has to be extended to the time domain, since deformation analysis implicitly needs to consider temporal correlations if they are existent. Therefore, the general ideas of modelling spatio-temporal correlations based on stochastic fields are presented. This will open the field for numerous possibilities to integrate modelled correlations into the deformation analysis process.

Keywords: Terrestrial laser scanning, correlation, synthetic covarinace matrix, stochastic field

Diese Veröffentlichung beschäftigt sich mit der wissenschaftlichen Untersuchung von Korrelationen beim terrestrischen Laserscanning. Sie fasst aktuelle Ansätze zur Korrelationsmodellierung, zur Entwicklung von Messszenarien zur empirischen Bestimmung von Korrelationen und zur Identifikation des Korrelationseinflusses auf diverse Schätzungsergebnisse zusammen. Es wird festgestellt, dass in den Bereichen vollständige synthetische Modellierung wie auch Entwicklung von Messszenarien zur empirischen Bestimmung von Korrelationen wesentliche Herausforderungen verbleiben. Des Weiteren ist für die Deformationsanalyse die Betrachtung auf die Dimension Zeit auszudehnen, da hier vorliegende zeitliche Korrelationen implizit zu berücksichtigen sind. Daher sind die grundlegenden Ansätze zur Modellierung raumzeitlicher Korrelationen auf Basis von Zufallsfeldern dargestellt. Dies eröffnet eine Vielzahl an Möglichkeiten zur Integration der so modellierten Korrelationen in den Deformationsanalyse-Prozess.

Schlüsselwörter: Terrestrisches Laserscanning, Korrelation, Synthetische Kovarianzmatrix, Zufallsfeld

1 INTRODUCTION

Terrestrial laser scanning (TLS) is one surveying method in engineering geodesy. It allows the acquisition of the complete surrounding automatically. Typical applications are among others industrial complexes, cultural heritage, building information modelling and tunnel surveys. Although the use of this technique is already wide-spread, some details with respect to the characteristics of the instrument as well as the resulting measurements are still unknown. This comprises the correction of the measurements for systematic effects such as the incidence angle effect, and knowledge about the stochastic relations among the measurements. These relations, the correlations, are the central topic of this contribution, since they play an essential part for computing correct variances of estimated quantities, like e.g. the radius of a sphere or a cylinder and for the correct statistical inference with respect to object deformations. As a typical example for this fact, /Holst & Kuhlmann 2014, 2015/ could not prove the statistical significance of areal-deformation of a radio telescope.

The remainder of the contribution is structured as follows. Section 2 gives an insight into modelling of correlations in engineering geodesy. Section 3 outlines the research related to synthetic modelling of correlations, whereas Section 4 does the same for their empirical determination and for the potential influence of correlations on estimated results. Section 5 gives an overview on stochastic fields and their potential applications in terrestrial laser scanning. Section 6 concludes the contribution.

2 CORRELATIONS IN GEODETIC METROLOGY

Engineering geodesy as well as metrology in general focuses on accurate and correct modelling of measurements. Systematic components have to be modelled functionally and, if possible, they should be corrected. Random components have to be modelled stochastically and are taken into account by using fully populated covariance matrices including correlations. Covariances as well as correlations may be determined empirically using real data or theoretically based on simulations and assumptions. In this contribution both possibilities are presented and discussed. In addition, the influence on the parameter estimation of geometric primitives is outlined.

Correlations may depend on the spatial distance d or on the time difference τ of two points or measurements. The spatial distance may be expressed using components like three Cartesian or polar coordinate component differences. In general, these correlations are called spatio-temporal correlations. In the context of terrestrial laser scanning, the temporal and the spatial components are interrelated, since the measurement process is realized in time and space domain simultaneously and, in the case of deformation measurements, space-related information may be linked in time due to (nearly) identical modelling approaches or environmental circumstances.

In probability theory as well as in geodesy, a measurement is regarded as a realization of a random variable Z. In case of multiple random variables, they form a random vector. Typical examples are the three coordinate components of a 3D position or all measurements of one laser scan. If the temporal component plays a role, a random vector may be available at defined points in time (epochs t) or even continuously. In these cases the random vectors, and therefore the random variables too, are arranged in random fields $Z(\boldsymbol{r}, t)$ where $\boldsymbol{r}$ defines the three dimensional space dependency. The spatio-temporal relationships among all variables are described by joint probability distributions. As written before, space and time are interrelated in the case of TLS.

/Matthias 1986/ already wrote about the importance of considering correlations in the field of metrology. The theoretic determination of correlations was introduced first by /Pelzer 1985/ using the model of elementary errors. /Augath 1985/ applied the model on distance measurement methods and /Heunecke 2004/ modelled total station measurements. /Schwieger 1999/ modelled correlations for GPS monitoring surveys and their influence on the results of deformation analysis. In his work the model of elementary errors was further expanded. Another model for a simulative correlation modelling is the Monte-Carlo-based procedure of the /GUM 2008a, 2008b/. /Koch 2008/ used e. g. rectangular and triangular probability distributions to model correlated output. /Koch et al. 2010/ also presented a method to determine variances and covariances between point coordinates by multiple TLS measurements on a static object. /Kutterer et al. 2010/ compared real and Monte-Carlo simulated measurements. They found that one of the TLS error sources, the angular increment of the servo-motor, has to be modelled using the rectangular instead of the Gaussian distribution, since for this appoach simulated and real measurements fitted together.

3 SYNTHETIC DETERMINATION OF CORRELATIONS

3.1 Synthetic Covariance Matrix

A synthetic covariance matrix reflects the impact of several error sources, considering non correlating impacts as well as correlating ones, on the variances, covariances and correlations within geodetic measurements, e. g. terrestrial laser scanning point clouds or GNSS observations. Regarding the requirements using this method the authors refer to e. g. /Pelzer 1985/.

By means of the elementary error model which is derived in detail in /Pelzer 1985/ and /Schwieger 1999/ a synthetic covariance matrix can be set up /Schwieger 2007/. According to the hypothesis of the elementary errors /Hagen 1837/, /Bessel 1837/ a random deviation is defined by a sum of many, very small elementary errors. On condition that each elementary error contains the same absolute value the probability of negative and positive sign might be equal. The assumption of an infinite number of elementary errors with infinitely small absolute values justifies the presumption of standard normal distribution. Modelling the impact on the observations requires error vectors as well as influencing matrices. The impact on the correlations within the point cloud can be modelled by using the functional relations between the elementary errors and the observations. In this approach three different types of impacts have to be considered: non-correlating errors ξ, functional correlating errors γ, and stochastic correlating errors δ. In order to determine influencing quantity values, an influencing matrix for each type is required as well as error vectors $\boldsymbol{\delta}_k$, $\boldsymbol{\xi}$, $\boldsymbol{\gamma}_h$ respectively. Hereby, the influencing matrices differ in their structures due to various effects of the elementary errors on the observations. Each elementary error of the non-correlating and stochastic correlating classes influences exactly one measurement quantity functionally which leads to diagonal matrices $\boldsymbol{D}_k$ and $\boldsymbol{G}_h$ (see Eq. (*1*)). By contrast, the matrix $\boldsymbol{F}$ is not structured diagonally, since each functional correlating error may affect more than one measurement quantity. For the purpose of illustration, the structures of the influencing matrices are shown below, where the elements of the matrices correspond to the partial derivatives of the functional relationships among elementary errors and observations with respect to the elementary errors:

$$\boldsymbol{D}_k = \begin{bmatrix} \frac{\partial \ell_1}{\partial \delta_{1k}} & 0 & \cdots & 0 \\ 0 & \frac{\partial \ell_2}{\partial \delta_{2k}} & 0 & \vdots \\ \vdots & 0 & \ddots & \vdots \\ 0 & \cdots & \cdots & \frac{\partial \ell_n}{\partial \delta_{nk}} \end{bmatrix}, \quad \boldsymbol{G}_h = \begin{bmatrix} \frac{\partial \ell_1}{\partial \gamma_{1h}} & 0 & \cdots & 0 \\ 0 & \frac{\partial \ell_2}{\partial \gamma_{2h}} & 0 & \vdots \\ \vdots & 0 & \ddots & \vdots \\ 0 & \cdots & \cdots & \frac{\partial \ell_n}{\partial \gamma_{nh}} \end{bmatrix},$$

$$\boldsymbol{F} = \begin{bmatrix} \frac{\partial \ell_1}{\partial \xi_1} & \frac{\partial \ell_1}{\partial \xi_2} & \cdots & \frac{\partial \ell_1}{\partial \xi_m} \\ \frac{\partial \ell_2}{\partial \xi_1} & \frac{\partial \ell_2}{\partial \xi_2} & \cdots & \frac{\partial \ell_2}{\partial \xi_m} \\ \vdots & \vdots & \ddots & \vdots \\ \frac{\partial \ell_n}{\partial \xi_1} & \frac{\partial \ell_n}{\partial \xi_2} & \cdots & \frac{\partial \ell_n}{\partial \xi_m} \end{bmatrix}. \tag{1}$$

As a result, the random deviation vector can be computed as follows:

$$\varepsilon = \sum_{k=1}^{p} \boldsymbol{D}_k \cdot \boldsymbol{\delta}_k + \boldsymbol{F} \cdot \boldsymbol{\xi} + \sum_{h=1}^{q} \boldsymbol{G}_h \cdot \boldsymbol{\gamma}_h. \tag{2}$$

Constructing a synthetic covariance matrix is based on the elementary error model. First, corresponding covariance matrices of the elementary errors have to be defined. The variances, each defining the stochastic variability of one random value, are placed on the main diagonal. The covariance between two observations is located on all off-diagonals. The matrices for the non-correlating errors, $\boldsymbol{\Sigma}_{\delta\delta,k}$, and for the functional correlating errors, $\boldsymbol{\Sigma}_{\xi\xi}$, are diagonal matrices (see Eq. (*3*)). By contrast, the covariance matrix of the stochastic correlating errors, $\boldsymbol{\Sigma}_{\gamma\gamma,h}$, may be fully populated due to covariances among the elementary errors of this type.

$$\boldsymbol{\Sigma}_{\delta\delta,k} = \begin{bmatrix} \sigma_{1k}^2 & 0 & \cdots & 0 \\ 0 & \sigma_{2k}^2 & 0 & \vdots \\ \vdots & 0 & \ddots & \vdots \\ 0 & \cdots & \cdots & \sigma_{nk}^2 \end{bmatrix}, \quad \boldsymbol{\Sigma}_{\xi\xi} = \begin{bmatrix} \sigma_1^2 & 0 & \cdots & 0 \\ 0 & \sigma_2^2 & \cdots & \vdots \\ \vdots & 0 & \ddots & \vdots \\ 0 & \cdots & \cdots & \sigma_m^2 \end{bmatrix},$$

$$\boldsymbol{\Sigma}_{\gamma\gamma,h} = \begin{bmatrix} \sigma_{1h}^2 & \sigma_{12h} & \cdots & \sigma_{1nh} \\ \sigma_{12h} & \sigma_{2h}^2 & \cdots & \sigma_{2nh} \\ \vdots & \vdots & \ddots & \vdots \\ \sigma_{1nh} & \cdots & \cdots & \sigma_{nh}^2 \end{bmatrix}. \tag{3}$$

Determining variances and covariances, in case of stochastic correlating errors for all groups of errors is challenging due to unknown correlations between the elementary errors. Thus, they may be specified either by using manufacturers' information, empirical values or by an estimation based on maximum errors or variance component estimation. In case the standard deviation is not known it may be derived by a maximum possible error and a probability distribution. For more details, the authors refer to /Schwieger 1999/.

Applying the law of error propagation on Eq. (*2*) leads to the equation of the synthetic covariance matrix:

$$\boldsymbol{\Sigma}_{\ell\ell} = \sum_{k=1}^{p} \boldsymbol{D}_k \cdot \boldsymbol{\Sigma}_{\delta\delta,k} \cdot \boldsymbol{D}_k^{\mathsf{T}} + \boldsymbol{F} \cdot \boldsymbol{\Sigma}_{\xi\xi} \cdot \boldsymbol{F}^{\mathsf{T}} + \sum_{h=1}^{q} \boldsymbol{G}_h \cdot \boldsymbol{\Sigma}_{\gamma\gamma,h} \cdot \boldsymbol{G}_h^{\mathsf{T}}. \tag{4}$$

3.2 Application of the Synthetic Covariance Matrix to Terrestrial Laser Scanning

In order to apply the synthetic covariance matrix to TLS point clouds, three sources of errors have to be considered: the manufacturing accuracy of the instrument itself, the atmosphere and the surface characteristics of the monitored object /Kauker & Schwieger 2015/. Grouping the elementary errors into instrumental, atmospheric and object based ones, simplifies the classification of the error sources regarding the three types of correlations mentioned in Section 3.1.

3.2.1 Elementary Errors of a Terrestrial Laser Scanner

Here it is assumed that the main error model of a terrestrial laser scanner is similar to that of a total station. The following instrumen-

tal errors are investigated: range noise and angular noise, scale error, zero point error, collimation axis error, horizontal axis error, vertical index error, tumbling error and eccentricity of the collimation axis. Range noise and angular noise are classified as non-correlated elementary errors while the remaining instrumental errors are grouped to the functional correlated group. Moreover, the functional relations between the instrumental errors and the observations are necessary in order to fill the influencing matrix. Details as well as numerical values for computing the matrices can be found in /Kauker & Schwieger 2016a/. /Holst & Kuhlmann 2016/ modelled different error sources that may reflect the functionality of the laser scanner using another construction model that may be more appropriate. For the current simulation the contribution considers the error sources described before.

3.2.2 Elementary Errors of the Atmosphere

Another main impact on the observations is caused by the atmosphere. Air temperature, air pressure and marginally also partial water vapour pressure affect the speed of propagation of the laser beam. Details regarding the functional model can be found in /Kauker & Schwieger 2015/. In general, these elementary errors are classified in the stochastic correlating group. Thanks to assumed homogeneous laboratory measurement conditions, the current analysis in Section 3.3. does not depend on the atmospheric influences on the laser signal path. This changes the elementary error from a stochastic to a functional correlating error type. Necessarily, the correlations become ±1 and the atmospheric elementary errors are modelled functionally /Kauker & Schwieger 2016a/. Each matrix $\boldsymbol{\Sigma}_{\gamma\gamma,h}$ including stochastic correlating errors then will be modelled as one variance in $\boldsymbol{\Sigma}_{\xi\xi}$ and the influences will be modelled as column of the matrix $\boldsymbol{F}$ instead of a complete matrix $\boldsymbol{G}_h$.

3.2.3 Elementary Errors based on the Monitored Objects

The third source of errors is defined by the surface quality and colour of the monitored objects. The intensity of the reflection of the laser beam on the object's surface depends mainly on reflectivity, roughness, colour, and penetration depth. Based on results from previous investigations the elementary errors are classified as stochastic correlating because they cannot be separated yet. Additionally, the angle of incidence influences the scanning result which is approximately modelled as functional error by means of Lambert's cosine law where the intensity of the reflected ray is proportional depending on the cosine of the angle of the incident ray /Kauker & Schwieger 2016b/.

3.3 First Synthetic Results

Having set all necessary parameters, the synthetic covariance matrix can be computed. The input values consist of a synthetic point cloud of 30 cm in length and 25 cm in width based on equivalent angle grid. The chosen point distance within the synthetic point cloud is at about 6 mm at the object and the scanning distance is up to 10 m. This is comparable to the resolution levels of the Leica HDS 7000 which served as an exemplary instrument. For evaluation the following standard deviations of instrumental errors are used.

Error source	Standard deviation
Range noise	0.5 mm
Angle noise	125 µrad
Scale error	0.300 018 mm/km
Zero point error	1.50 mm
Collimation axis error	0.44 mgon
Horizontal axis error	0.48 mgon
Vertical index error	0.53 mgon
Tumbling error	0.06 mm/m
Eccentricity of the collimation axis	0.08 mm

Tab. 1 | Standard deviations of instrumental errors

For first investigations, the atmospheric parameters must be adjusted to the laboratory conditions by taking into account that the variances and covariances are not dependent on their location due to the small dimensions of the sample pieces. Subsequently, the standard deviations for temperature, pressure and partial water vapour pressure are set to $\sigma_t = 0.01$ °C, $\sigma_p = \sigma_e = 0$ hPa, respectively. With the structure of the synthetic covariance matrix (see Eq. (*5*)), a position error can be calculated as the square root of the sum of the respective three coordinate-related variances /Kauker & Schwieger 2016a/.

$$\boldsymbol{\Sigma}_{\ell\ell} = \begin{bmatrix} \sigma_{x_1}^2 & \sigma_{x_1 y_1} & \sigma_{x_1 z_1} & \cdots & \sigma_{x_1 z_n} \\ \sigma_{x_1 y_1} & \sigma_{y_1}^2 & \sigma_{y_1 z_1} & & \\ \sigma_{x_1 z_1} & \sigma_{y_1 z_1} & \sigma_{z_1}^2 & & \vdots \\ \vdots & & & \ddots & \\ \sigma_{x_1 z_n} & & \cdots & & \sigma_{z_n}^2 \end{bmatrix} \tag{5}$$

As a result, the positional standard deviation reaches 3.9 mm over the entire area due to the small impacts of elementary errors caused by the small size of the grid as well as neglecting atmospheric and object based impacts. In the next step, the correlation matrix $\boldsymbol{R}_{\ell\ell}$, containing spatial correlations within the point cloud, can be computed by means of a synthetic covariance matrix. Due to its structure, that is equal to the one of $\boldsymbol{\Sigma}_{\ell\ell}$, correlations for each coordinate axis can be calculated directly. A more thorough analysis shows a tiny trend regarding the spatial correlations of the *x*-coordinates which depends on the distances to each other (see *Fig. 1*). With respect to the scanning setup the *x*-axis defines the collimation axis, the *z*-axis represents height and the *y*-axis is orthogonal to both axes. For the other coordinates approximately the same picture results. Moreover, the results heavily depend on the scanning resolution and the distance between laser scanner and object. If the size of the object increases also smaller correlations will appear. The non-changing variances as well as the high correlations are caused by the major influence and the low variability of the instrumental

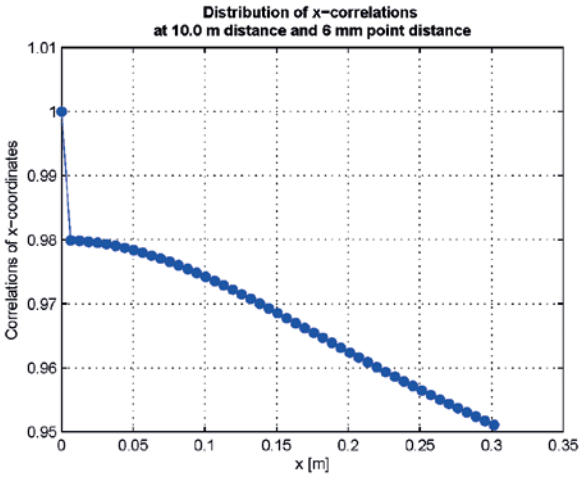

Fig. 1 | Correlations of x-coordinates depending on their spacing

errors, the unchanged atmospheric conditions, and the symmetric geometry of the configuration of the work piece.

3.4 Recent Challenges

Currently, the synthetic covariance matrix was determined for small work pieces under laboratory conditions. This has to be expanded to larger objects such as buildings, industrial structures, bridges or dams. In this case the atmospheric errors as well as the instrumental and the object-related errors will have a larger influence. Defining variances and covariances for the stochastic correlating group for the atmospheric errors is one of the most challenging parts of the future modelling. Additionally, for the object-related errors no strict functional relations regarding reflectivity, colour, penetration depth and roughness are known yet. However, modelling the effect of the angle of incidence is challenging as well due to the object characteristics which affect the intensity of the laser beam simultaneously. Most of these dependencies are and will be modelled by stochastical correlating errors, too.

In addition, the synthetic covariance matrices have to be verified or validated by empirically determined variances, covariances and correlations. Here, the difficulty of taking all possible error sources into account has to be solved. Some recent ideas are documented in the following section.

4 EMPIRICAL DETERMINATION OF CORRELATIONS AND THEIR INFLUENCE ON ESTIMATIONS

The empirical determination of correlations is divided into two parts. The first one concerns the empirical determination of correlations to validate the synthetic correlations simulated in Section 3. The second part deals with finding sophisticated test scenarios that help revealing existing correlations of laser scans.

4.1 Empirical Determination of Correlations

Validating the synthetic covariance matrix requires an empirical determination of the variance covariance matrix of the observations. For this purpose, multiple scans can be used, directly carried out after one another, to justify the assumption of no changes in the scanning process, respectively of the environmental influences. Determining a variance covariance matrix for empirical measurements requires identical points measured in different epochs. However, regarding the angular variability being dominated by the true horizontal and vertical angle as well as different starting points of scans, each point cloud is unique; the scanner will not measure the same points in two scans. Thus, it is not possible to identify the same point in different point clouds reliably.

In order to identify almost identical points, algorithms of pattern recognition can be used. Here the k-nearest-neighbour-algorithm /Geisselmann 1981/ is applied. Having found "almost identical points", residuals $\boldsymbol{v}$ for each observation l_{ij} can be computed:

$$v_{ij} = l_{ij} - \overline{l_{ij}}, \text{ with } i = 1, 2, \ldots, n \text{ and } j = 1, 2, \ldots, m. \quad (6)$$

n defines the number of measurements per point and m the number of points in the point cloud. Afterwards, an empirical covariance matrix $\boldsymbol{S}_{\ell\ell}$ can be determined as follows, where v_j, v_k define vectors of the residuals for one point j respectively k:

$$\boldsymbol{S}_{\ell\ell} = \frac{1}{n-1} \sum_{j,k=1}^{n} \boldsymbol{v}_j \boldsymbol{v}_k. \quad (7)$$

It is clear, that due to the angular variability and different starting points of the scanner the empirical variation does not contribute to the uncertainty of the coordinates of the points in the point clouds. Nevertheless, as a first approach almost identical points are identified in order to compute an empirical variance covariance matrix.

As described in Section 3.2 for the theoretical correlation matrix an empirical correlation matrix can be calculated in the following.

For first measurements the terrestrial laser scanner Leica HDS 7 000 is used. A small sample piece made of gypsum by a 3D printer is scanned. This material is used for testing purposes, in order to investigate its reflectivity. The dimensions of the board are approximately 30 cm x 25 cm x 0.4 cm. The board is placed 10 m in front of the laser scanner. The scanning resolution is 0.036° whereof a point distance of 6 mm within the point cloud results. By applying the variances the empirical position error (according to Helmert) can be calculated for each point within the cloud /Pelzer 1985/:

$$s_{xyz_i} = \sqrt{s_{x_i}^2 + s_{y_i}^2 + s_{z_i}^2}, \; i = 1, \ldots, m. \quad (8)$$

Fig. 2 shows the result of the calculation of the three dimensional positional error which is mainly up to 1.3 mm within the surface. Nevertheless, the lower and upper edges cause values up to 5 mm standard deviation assumingly caused by the nearest-neighbour-algorithm. These values represent the dominating impact of noise on the measurements and some influences of the non-identical points. Moreover, the empirical residuals are smaller than the noise modelled in Section 3. The visible pattern is assumed to be caused by the rough surface structure.

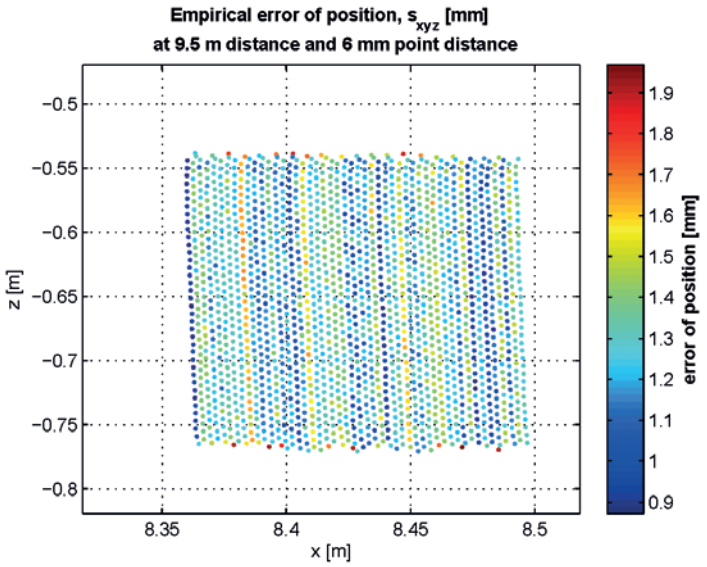

Fig. 2 | Empirical positional standard deviations

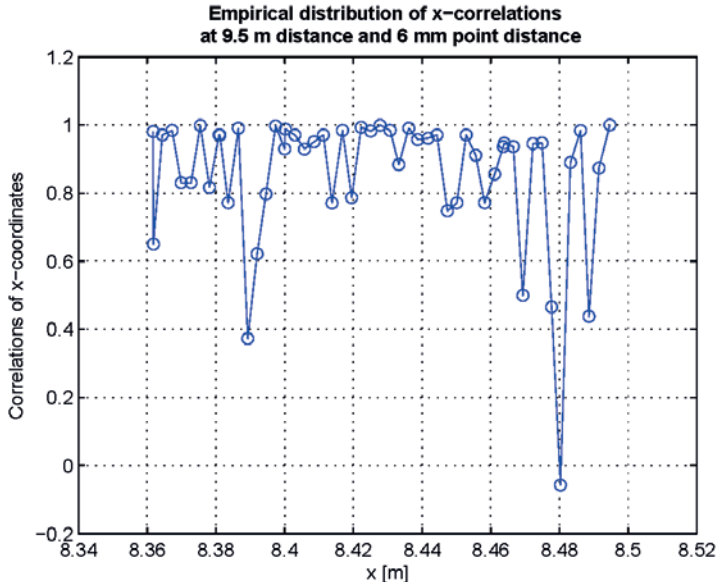

Fig. 3 | Empirical correlations of x-coordinates

Fig. 3 explores the empirical correlations with respect to the *x*-coordinates which range between −0.1 and +1. Due to the dominating influence of the range noise as well as the result of the angular variability during the scanning process the correlations vary between −1 and +1 across the entire surface.

This irregular pattern clearly reflects that these first results cannot be used for a scientific analysis and interpretation. The complete empirical determination is an open research question developing specific measurement configurations.

Consequently, for understanding the amount and the sources of correlations in laser scanning, sophisticated test scenarios have to be developed that aim at revealing correlations empirically to build up a covariance matrix as written in Eq. (*4*)[1]. The setting up of a suited test scenario is closely related to the type of elementary errors that is considered. Hence, it differs between aiming at

[1] The setting up of such a test scenario is not trivial; it is stated as a recent challenge in Section 4.3.

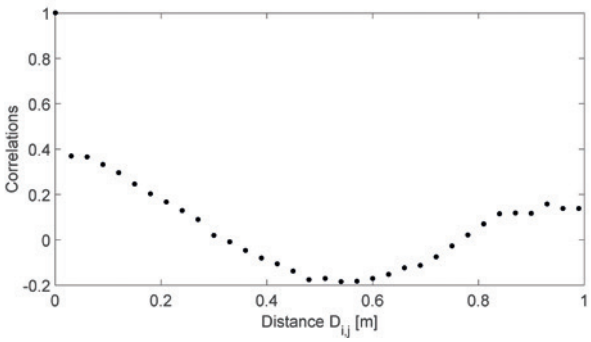

Fig. 4 | Estimated correlations between the residuals of the scan points (after fitting a plane) depending on their distance /Jurek 2015/

revealing fundamental errors of the terrestrial laser scanner, the atmosphere or the monitored object that all can be functional or stochastic correlating (see Section 3.2).

A special scenario described in the following deals with revealing fundamental errors of the monitored object which are assumed to be stochastic correlating. In this test, a wooden plate of 1.5 m width and height is scanned from 7 m distance /Jurek 2015/. This scan is afterwards parameterized as a plane and the relevant parameters (normal vector and distance) are estimated in a least-squares surface estimation similar to /Holst et al. 2014/. This procedure is partially analogous to /Koch 2008/ and /Koch et al. 2010/ who investigated temporal correlations in laser scans.

Correlations can be estimated afterwards based on the estimated residuals. These correlations are displayed in *Fig. 4* depending on the distance between the scan points corresponding to *Fig. 1*. It can be seen that these correlations of up to 0.40 are decreasing with increasing point distance. This decrease is expectable since the stochastic relationships investigated here depend on the spatial distance between the points (see Section 2).

However, the correlations do not decrease to zero; instead, some systematic characteristic can be seen. Further investigations show that the scanned wooden plate is not absolutely planar but slightly curved /Jurek 2015/. Hence, the correlations shown in *Fig. 4* are due to laser scanner (co-)variances as well as to an insufficient functional model in the adjustment, since this functional model assumes the plate to be planar. Consequently, the quantification shown in *Fig. 4* should be handled critically because it contains laser scanner correlations as well as unknown areal deformations of the scanned surface.

4.2 Influence of Correlations on the Estimation

As already mentioned, spatio-temporal correlations in terrestrial laser scanning data are mostly unknown. Thus, they cannot be included in the stochastic model when approximating the scan by some areal model based on a least-squares estimation. Hence, when building the covariance matrix of the observations $\boldsymbol{\Sigma}_{\ell\ell}$ for real applications, only the main diagonal axis is filled, the other elements are empty due to lack of knowledge. Since this does not

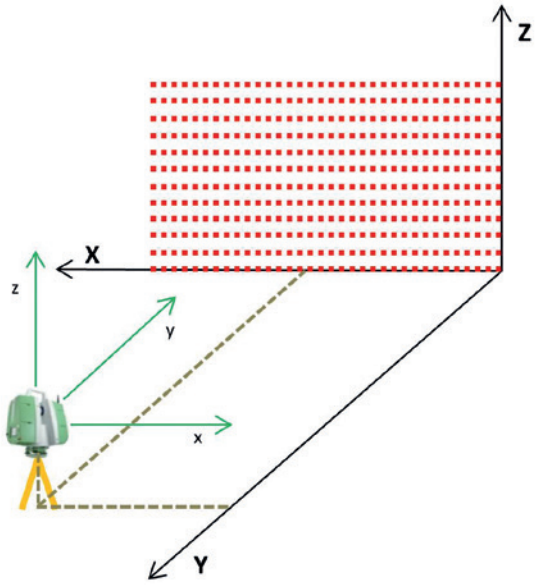

Fig. 5 | Configuration of simulated plane and laser scanner station

reflect the real situation, the effect of the simplified stochastic model on the estimated parameters $\hat{\boldsymbol{x}}$ and the corresponding covariance matrix $\boldsymbol{\Sigma}_{\hat{x}\hat{x}}$ should be investigated. This can be done by the parameter test e. g. /Niemeier 2007/ if the true parameters of the adjustment $\boldsymbol{x}$ are known:

$$T = \frac{1}{u}(\hat{\boldsymbol{x}}-\boldsymbol{x})^{\mathrm{T}}\,\boldsymbol{\Sigma}_{\hat{x}\hat{x}}^{-1}\,(\hat{\boldsymbol{x}}-\boldsymbol{x}) \sim \mathfrak{F}_{u,f,1-\alpha}. \tag{9}$$

Here, the $\mathfrak{F}$-distribution is based on the number of parameters u, the degrees of freedom f and the significance level α. This test indicates whether the estimated parameters differ significantly from the true ones with respect to the corresponding covariance matrix. Hence, it detects a bias in the estimation assuming that the stochastic model is correct.

The following investigations are based on simulations /Jurek 2015/ (see *Fig. 5*): The laser scanner is stationed in 10 m distance of a wall of 1 m width and height. The polar observations of the laser scanner are generated based on analytical geometry and simulated errors are added afterwards. Based on these observations, the parameters of the planar wall (normal vector and distance) are estimated in a least-squares surface estimation similar to /Holst et al. 2014/.

In the present case, only non-correlating errors are incorporated for the angle measurements. They shall represent the measurement noise. For the distance measurements, stochastic correlating errors are additionally incorporated. They model the elementary errors of the monitored object due to reflectivity, roughness, colour and penetration (compare Section 3.2). Functional correlating errors as the ones due to the imperfection of the instrument are not considered in this analysis. This step is left for future research.

The incorporated stochastic correlating errors are assumed to lead to correlations R_{ij} between the scan points i and j that decrease with increasing point distance D_{ij}. This can be described by the exponential function

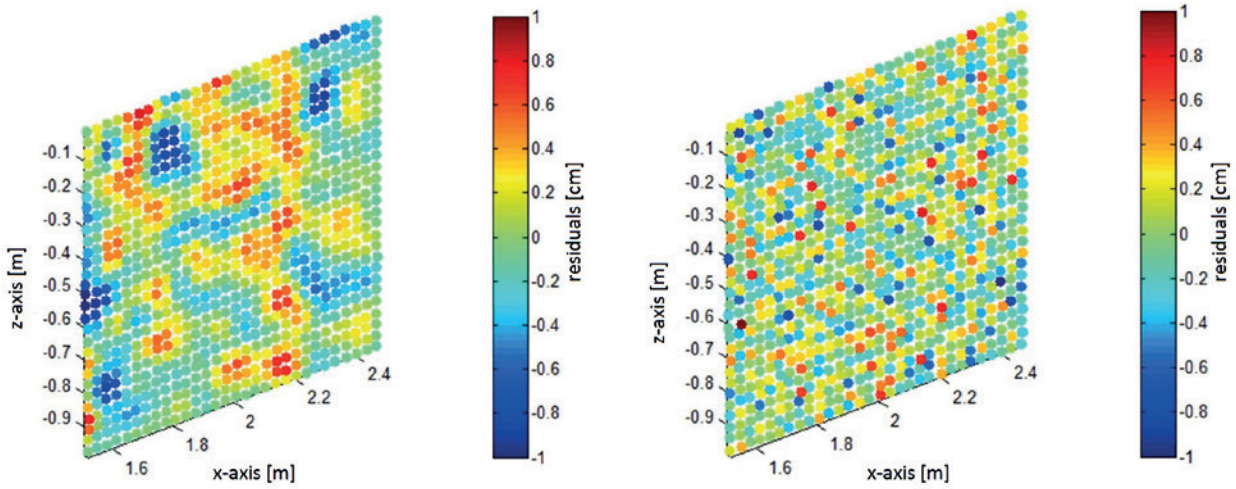

Fig. 6 | Residuals of distance measurements of a plane approximation in case of only non-correlating errors (right) and in case of non-correlating as well as stochastic correlating errors (left) /Jurek 2015/

$$R_{ij} = R\left(D_{ij}\right) = \mathrm{e}^{-\frac{1}{2}\left(\frac{D_{ij}}{D_0}\right)^2}, \tag{10}$$

with D_0 defining the correlation length. The combination of all correlations R_{ij} builds up the correlation matrix $\boldsymbol{R}_{\ell\ell}$ that has already been introduced in Section 3.3. *Fig. 6* shows the effect of incorporating only non-correlating errors (right) and of additionally incorporating stochastic correlating errors (left) corresponding to the correlation matrix $\boldsymbol{R}_{\ell\ell}$.

The influence of the correlations on the parameter estimation can now be investigated by a two-step analysis: In the first step, although stochastic correlations are incorporated in the simulation of the observations, they are assumed to be unknown in the stochastic model. Hence, still only the main diagonal of $\boldsymbol{\Sigma}_{\ell\ell}$ is filled since $\boldsymbol{\Sigma}_{\delta\delta,k}$ is filled but $\boldsymbol{\Sigma}_{\xi\xi}$ and $\boldsymbol{\Sigma}_{\gamma\gamma,h}$ are not (see Eq. (*3*)). This part reflects the present procedure of approximating laser scans because the existing correlations are indeed unknown in most applications. Hence, this first step is called "present case". In the second step, stochastic correlations are incorporated in $\boldsymbol{\Sigma}_{\ell\ell}$ by additionally filling $\boldsymbol{\Sigma}_{\gamma\gamma,h}$ based on $\boldsymbol{R}_{\ell\ell}$ which is possible since these correlations are simulated. This part indicates the benefit of the efforts of building up a synthetic covariance matrix for laser scanning. This step is called "desired case".

Consequently, it can be analysed (i) whether the parameter test (Eq. (*9*)) is declined if the true stochastic model including correlations

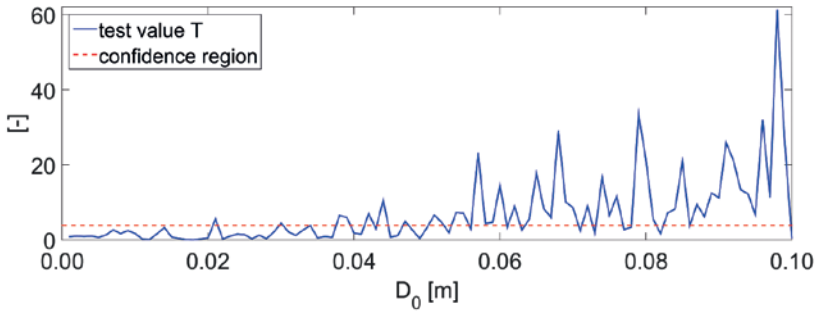

Fig. 7 | "Present case": Results of the parameter test in several simulation runs dependent on the correlation length D_0 /Jurek 2015/

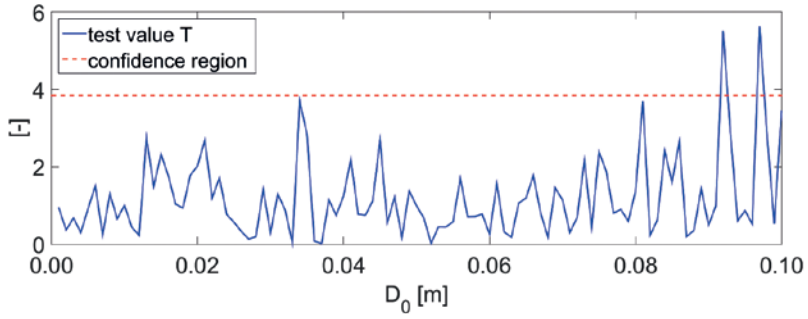

Fig. 8 | "Desired case": Results of the parameter test in several simulation runs dependent on the correlation length D_0 /Jurek 2015/

is unknown ("present case") and (ii) whether the parameter test is accepted if the true stochastic model would be known ("desired case"). Hence, these analyses investigate whether a more realistic stochastic model for terrestrial laser scanning affects a potential parameter bias at approximating scanned surfaces.

Fig. 7 shows the results for the "present case" for several simulation runs dependent on the correlation length D_0 (see Eq. (*10*)). It can be seen that the parameter test indicates the wrong stochastic model with increasing correlation length. Thus, neglecting correlations at laser scanning leads to a biased parameter estimation. This bias depends on the true correlation length that is not yet known; or more generally: it depends on the correct size of the correlations and their spatio-temporal behaviour.

Fig. 8 shows the results for the "desired case": Here, the correlations are known and, thus, the test statistics are accepted independent from the correlation length. The test is declined only twice which corresponds to the significance level.

These investigations imply that gaining a more realistic stochastic model – especially regarding spatio-temporal correlations – eliminates the bias in surface approximations based on laser scans. Without incorporating existing correlations in the covariance matrix of the observations $\boldsymbol{\Sigma}_{\ell\ell}$, the parameter test is rejected because the items of the estimated covariance matrix of the parameters $\boldsymbol{\Sigma}_{\hat{x}\hat{x}}$ are too small (see Eq. (*9*)), since $\boldsymbol{\Sigma}_{\hat{x}\hat{x}}$ is a result of the covariance propagation of $\boldsymbol{\Sigma}_{\ell\ell}$. Consequently, the main reason for the decline of the parameter test in the "present case" – indicating that the estimation is biased – can be found in the too optimistically estimated covariance matrix $\boldsymbol{\Sigma}_{\hat{x}\hat{x}}$ not reflecting the true stochastic behavior of the parameters $\hat{\boldsymbol{x}}$. Hence, a more realistic stochastic model for laser scanning including correlations is needed to improve the parameter estimation.

4.3 Recent Challenges

The previous Sections 4.1 and 4.2 demonstrate that the empirical determination of laser scanner correlations is very complex (see also /Holst & Kuhlmann 2016/): while some studies have already proven the existence of correlations, general strategies for revealing and assessing correlations are not at hand. This task is challenging since these correlations presumably differ by a large amount between different measurement configurations and scanned objects.

The challenge of empirically revealing correlations in laser scans is bound to the fact that a very accurately known surface has to be scanned. Even small unknown deformations of this surface lead to falsely assumed correlations (see Section 4.2). However, even if this surface can be parameterized accurately, the empirically estimated correlations might then only be representative for this specific surface and measurement configuration.

Consequently, several test scenarios need to be build up. Then, the estimated correlations might still only be valid for each specific combination of scanned object and measurement configuration but the aggregation of several scenarios could improve the general comprehension about spatio-temporal correlations at laser scanning. This could lead – in whole – to a more realistic empirical determination of the synthetic covariance matrix presented in Section 3.

5 SPATIO-TEMPORAL STOCHASTIC FIELDS

In addition to the previous approaches, concepts from spatio-temporal data analyses can be used to describe the stochastics of laser scanner data in four dimensions. Here, the basic idea is that the data set is a realisation of a stochastic process, this process is characterised by its spectrum or covariance function. Useful references for spatio-temporal processes are /Cressie 1993/, /Cressie & Wikle 2011/ or /Schabenberger & Gotway 2005/. In geodesy, these concepts have been introduced and used in different contexts: /Grafarend 1976/ gave a general overview, /Illner & Müller 1984/ applied concepts in geodetic network optimisation when using criterion matrices of Taylor-Karman type, /Schön & Brunner 2008/ and subsequent publications like /Schön & Kermarrec 2015/ or /Kermarrec & Schön 2014/ proposed stochastic models for GNSS. Finally, these concepts are applied in modern image processing as conditional random fields, e. g. /Förstner 2013/ for an overview.

5.1 Methodical Basics

One powerful family of covariance functions that is widely used is the Matern family. The spatial covariance function C_S of the field Z between two distinct points $\boldsymbol{r}$ and $\boldsymbol{r}+\boldsymbol{d}$ in space reads

$$C_S\left(Z(\boldsymbol{r}), Z(\boldsymbol{r}+\boldsymbol{d})\right) = A\left(\alpha\left\|\boldsymbol{d}\right\|\right)^{\nu} K_\nu\left(\alpha\left\|\boldsymbol{d}\right\|\right), \tag{11}$$

where A is a constant, α the inverse correlation length, and ν a positive constant that describes the smoothness of the field, i. e. the rate of decay of the spectral density at high frequencies or equivalent the steepness of the departure of the covariance function from 0. Finally, K_ν denotes the modified Bessel function of the second kind (MacDonald function). *Fig. 9* illustrates the covariance function for different parameter sets. The exponential model is obtained by $\nu = 1/2$ and the Gaussian case considered in Section 4 when $\nu \to \infty$.

The covariance function from Eq. (*11*) describes homogeneous and isotropic fields, i. e. the covariance is independent of the direction of $\boldsymbol{d}$ and the location $\boldsymbol{r}$; it depends only on the length $\left\|\boldsymbol{d}\right\|$ of $\boldsymbol{d}$. Subsequently, the associated variance-covariance matrix $\boldsymbol{\Sigma}$ has a Toeplitz structure. This could be a simple model for TLS data where $\left\|\boldsymbol{d}\right\|$ is the distance between scan points. Its elements σ can be computed by Eq. (*11*).

If needed, anisotropy and inhomogeneity can be introduced to first order by an affine transformation of the coordinate system, i. e. a rotation by β and a scaling of the rotated axes by a and b, respectively:

$$\boldsymbol{r}' = \boldsymbol{B}\,\boldsymbol{r} = \begin{bmatrix} 1/a & 0 \\ 0 & 1/b \end{bmatrix} \begin{bmatrix} \cos\beta & -\sin\beta \\ \sin\beta & \cos\beta \end{bmatrix} \boldsymbol{r}. \tag{12}$$

Up to now, just spatial correlations are treated. The link between temporal and spatial correlations can be introduced in different ways: In a first approach, separable processes can be assumed. Then, the spatio-temporal variation of the field Z can be described by the product of two covariance functions, C_S considering exclusively the spatial covariance and C_T only the temporal covariance, respectively:

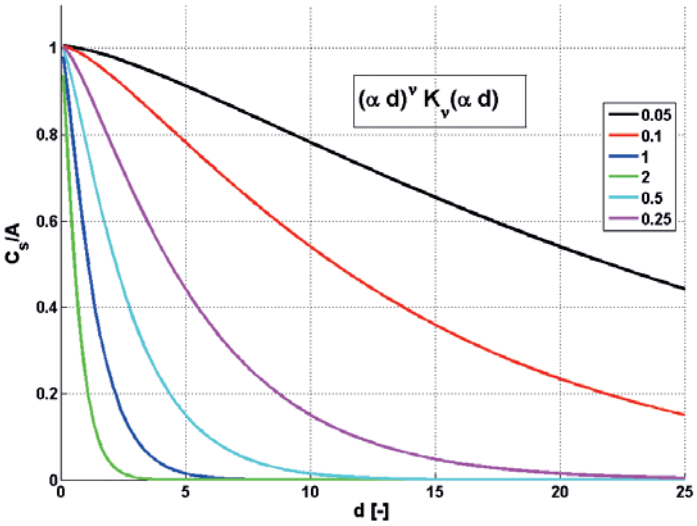

Fig. 9 | Representation of the Matern family for different values of ν when the correlation length is fixed (here $\alpha = 1$)

$$C_{ST}\left(Z\left(\boldsymbol{r},t\right),Z\left(\boldsymbol{r}+\boldsymbol{d},t+\tau\right)\right)=C_S\left(Z\left(\boldsymbol{r}\right),Z\left(\boldsymbol{r}+\boldsymbol{d}\right)\right)C_T\left(t,t+\tau\right). \quad (13)$$

Alternatively, the sum or a combination of sum and product is also feasible. Special attention should be paid to the anisotropy of space and time in these formulations. In addition, actually not all processes show this behaviour, cf. /Cressie & Wikle 2011, p. 308 ff./.

A second approach is based on Taylor's frozen turbulence hypothesis, often applied in turbulence theory. Here, the spatial random structure is assumed to be frozen and temporal variations are included by transporting this frozen field in space with a constant velocity vector $\boldsymbol{u}$, i.e. a "wind" vector. Thus, $C_{ST}\left(Z\left(\boldsymbol{r},t\right),Z\left(\boldsymbol{r},t+\tau\right)\right)=C_{ST}\left(Z\left(\boldsymbol{r},t\right),Z\left(\boldsymbol{r}+\boldsymbol{u}\tau,t\right)\right)$, i.e. the covariance between values at the same position at different epochs separated by τ is identical with the covariance at the same epoch but at positions separated by $\boldsymbol{u}\tau$.

$$C_{ST}\left(Z\left(\boldsymbol{r},t\right),Z\left(\boldsymbol{r}+\boldsymbol{d},t+\tau\right)\right)=C_S\left(Z\left(\boldsymbol{r}\right),Z\left(\boldsymbol{r}+\boldsymbol{d}+\boldsymbol{u}\tau\right)\right). \quad (14)$$

A random field can be generated by eigenvalue decomposition of the covariance matrix: $\boldsymbol{\Sigma}=\boldsymbol{M}\,\boldsymbol{\Lambda}\,\boldsymbol{M}^T$, where $\boldsymbol{M}$ is the orthonormal modal matrix containing the eigenvectors and $\boldsymbol{\Lambda}$ the diagonal matrix of decreasingly ordered eigenvalues. Then, with a normal distributed random vector $\boldsymbol{n}$, the random field Z can be generated by

$$Z\left(\boldsymbol{r},t\right)=\boldsymbol{M}\,\boldsymbol{\Lambda}^{\frac{1}{2}}\,\boldsymbol{n}\;=\;\sum_{i=1}^{2npt}\boldsymbol{m}_i\sqrt{\lambda_i}\,n_i\,. \quad (15)$$

The right hand side of Eq. (*15*) shows that the field is a superposition of the structures given in the eigenvectors $\boldsymbol{m}_i$. The weights are the corresponding eigenvalue $\sqrt{\lambda_i}$ and the random number $\boldsymbol{m}_i$. In the case of Toeplitz like matrices the eigenvectors contain the principal modes of an oscillation, cf. *Fig. 10* (right).

A second benefit of eigenvalue decomposition is the assessment of data weak forms similar to weak forms known from geodetic network analyses, cf. /Jäger 1988/. Weak forms are obtained if few eigenvalues are dominating the eigenvalue spectrum. In these cases the structure of the field obtained by the associated eigenvectors determines deformations that are difficult to be detected due to the correlations.

Fig. 10 (above left) shows the resulting random field at 25 × 25 positions for the case of anisotropy, cf. Eq. (*11*). The rotated coordinate system is associated

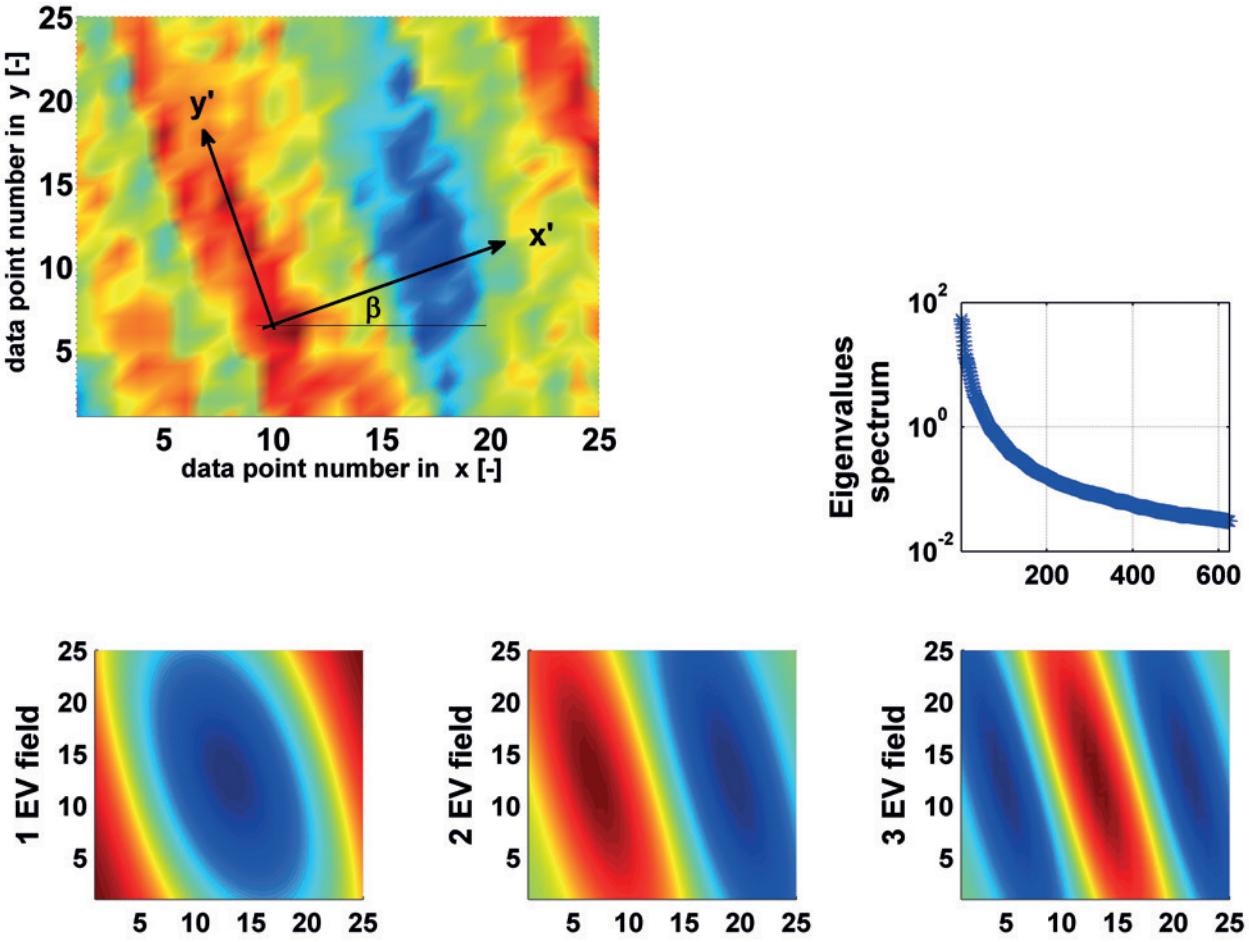

Fig. 10 | Simulated random field. Above left: Field at 25 x 25 data points assuming anisotropy ($a = 0.1$, $b = 1$, $\beta = 15°$, $\nu = 5/6$, $\alpha = 0.1$). Bottom: Spectrum and contributions to the field given by the eigenvectors

with the structures generated in the field. Since a is smaller than b in this specific example the correlation in y'-direction is larger than in x'-direction. In subfigure 10 (further down) the eigenvalue decomposition of the 625 × 625 fully populated covariance matrix is depicted. The spectrum of eigenvalues is relatively flat, so that no dominant eigenvalues can be stated. The structure of the first three eigenvectors shows a typical oscillation pattern which is due to the Toeplitz-like variance-covariance matrix. The structures associated with the smaller eigenvalues shows rather random patterns. Here we plotted exemplarily the fields associated with eigenvalues 100, 500, and the smallest eigenvalue 625 were plotted.

Fig. 11 illustrates the principle of taking spatial and temporal correlations into account, the latter by Taylor's frozen hypothesis. Here a field of 20 × 20 data points is generated using the Matern covariance function with $\nu = 5/6$ and $\alpha = 0.001$, $a = 1$, $b = 0.1$, and $\beta = 15°$. This field is transported by the wind vector $\boldsymbol{u} = 10$ m/s. Subsequently, at epoch t_2 the segment B1 of the initial field is now located at the segment B2. A new data structure was transported into the segment C2. Consequently, Taylor's hypothesis could be interesting when observing transport or similar structured processes with laser scanning.

5.2 Applications for terrestrial laser scanning

Sections 3 and 4 have dealt with the challenges of modelling, generating and determining correlations within one laser point cloud, partly based on successive laser scans of the same object. These modelling and analysis approaches deal with the spatial part of the correlations. Nevertheless any scan process automatically deals with time concurrently, since the points cannot be acquired at the same time. So each point shows another position as well as another point of time when acquired by TLS. Time and space is related by the measurement principle of the instrument. Here the simple integration of temporal and spatial correlations as indicated in Eq. (*13*) can probably not be followed. The theory of stochastic fields has to be studied more in detail and adequate solutions have to be developed for application to TLS.

Monitoring and deformation analysis in particular is an important application in engineering geodesy. Therefore, time is always an important issue. /Schwieger 1999/ analysed temporal correlations for GPS monitoring surveys. For the modelling he needed the spatial correlation component, too. He referred to stochastic fields in the simple form separating between the spatial and time domain as

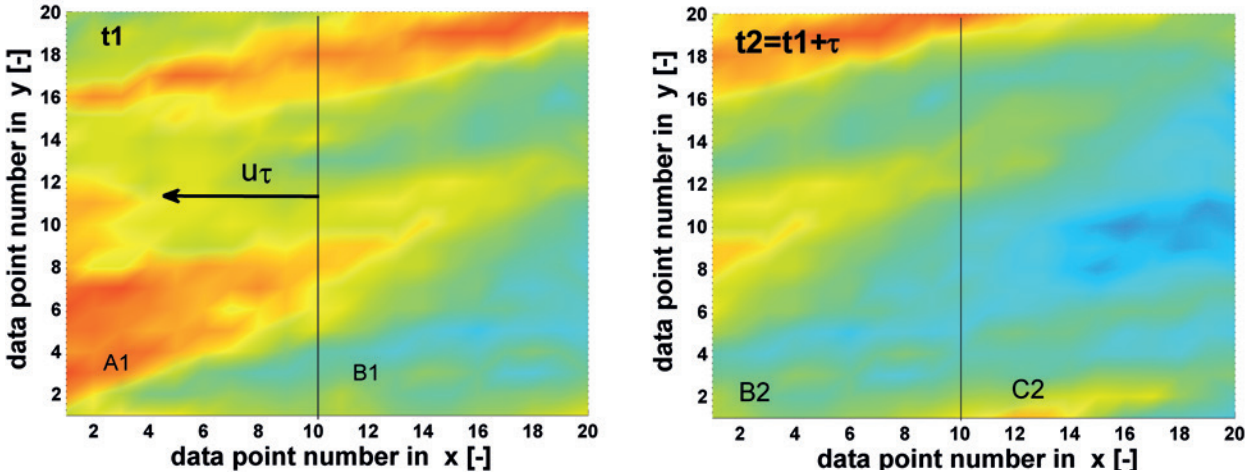

Fig. 11 | Temporal variations of a random field by Taylor's frozen hypothesis.
Left: Field with 20 × 20 data points at epoch t_1. A wind vector u is transporting the field. Right: Resulting field at epoch t_2.

described in Eq. (*13*). For deformation analysis of laser scanner point clouds the complexity with respect to spatial correlations and to the interaction of space and time is much higher. Approaches described in Section 5.1 deliver the theoretical background for adapted (approximated) four-dimensional correlation models.

6 CONCLUSION AND OUTLOOK

This contribution summarizes the difficulties and importance of modelling correlations in terrestrial laser scanning on the scientific level. It focuses on recent approaches to model correlations, to develop measurement scenarios for the determination of correlations as well as to identify the influence of the correlations on estimation procedures. It can be concluded that challenges are remaining, concerning the complete synthetic modelling as well as concerning the development of appropriate measurement scenarios to determine correlations in an empirical way. Additionally, the research has to be extended to the time domain, since deformation analysis implicitly needs to consider temporal correlations if they are available. Therefore, the general ideas of modelling spatio-temporal correlations on the base of stochastic fields are presented. This will open the field for numerous possibilities to integrate modelled correlations into the deformation analysis process.

REFERENCES

Augath, W. (1985): Lagenetze. In: Pelzer, H. (Ed.): Geodätische Netze in Landes- und Ingenieurvermessung. Wittwer, Stuttgart.

Bessel, F. W. (1837): Untersuchungen über die Wahrscheinlichkeit der Beobachtungsfehler. In: Astronomische Nachrichten, 15(1837), 369–404.

Cressie, N. (1993): Statistics for spatial data. 2nd rev. Ed. John Wiley & Sons, New York.

Cressie, N.; Wikle, C. K. (2011): Statistics for spatio-temporial data. John Wiley & Sons, New York.

Förstner, W. (2013): Graphical Models in Geodesy and Photogrammetry. In: Photogrammtrie – Fernerkundung – Geoinformation (PFG), 2013(4), 255–267.

Geisselmann, H. (1981): Bildsensor zur Mustererkennung und Positionsmessung bei programmierbaren Handhabungsgeräten. Springer, Berlin.

Grafarend, E. W. (1976): Geodetic applications of stochastic processes. In: Physics of the Earth and Planetary Interiors, 12(1976)2-3, 151–179.

GUM (2008a): JCGM 100:2008: Uncertainty of measurement – Part 3: Guide to the expression of uncertainty in measurement.

GUM (2008b): JCGM 101:2008: Supplement 1 to the "Guide to the expression of uncertainty in measurement" – Propagation of distributions using a Monte Carlo method.

Hagen, G. (1837): Grundzüge der Wahrscheinlichkeits-Rechnung. F. Dümmler, Berlin.

Heunecke, O. (2004): Nochmals über Korrelationen in der Messtechnik. In: Festschrift Univ.-Prof. Dr.-Ing. habil. Dr. h. c. mult. Hans Pelzer zum 68. Geburtstag. Wissenschaftliche Arbeiten der Fachrichtung Vermessungswesen der Universität Hannover, 250(2004), 91–108.

Holst, C.; Artz, T.; Kuhlmann, H. (2014): Biased and unbiased estimates based on laser scans of surfaces with unknown deformations. In: Journal of Applied Geodesy, 8(2014)3, 169–183.

Holst, C.; Kuhlmann, H. (2014): Aiming at self-calibration of terrestrial laser scanners using only one single object and one single scan. In: Journal of Applied Geodesy, 8(2014)4, 295–310.

Holst, C.; Kuhlmann, H. (2015): Improved area-based deformation analysis of a radio telescope's main reflector based on terrestrial laser scanning. In: Journal of Applied Geodesy, 9(2015)1, 1–14.

Holst, C.; Kuhlmann, H. (2016): Challenges and present fields of action at laser scanner based deformation analyses. In: Journal of Applied Geodesy, 10(2106)1, 17–25.

Illner, M.; Müller H. (1984): Gewichtsoptimierung geodätischer Netze. Zur Anpassung von Kriteriumsmatrizen bei der Gewichtsoptimierung. In: Allgemeine Vermessungs-Nachrichten (AVN), 91(1984)7, 253–269.

Jäger, R. (1988): Analyse und Optimierung geodätischer Netze nach spektralen Kriterien und mechanische Analogien. Deutsche Geodätische Kommission, Reihe C, 342. Munich.

Jurek, T. (2015): Analyse von Korrelationen beim terrestrischen Laserscanning. Master's Thesis, Institute of Geodesy and Geoinformation, University of Bonn (unpublished).

Kauker, S.; Schwieger, V. (2015): Approach for a Synthetic Covariance Matrix for Terrestrial Laser Scanner. Proceedings of 2nd International Workshop on Integration of Point- and Area-wise Geodetic Monitoring for Structures and Natural Objects, March 23–24, 2015, Stuttgart, Germany.

Kauker, S.; Schwieger, V. (2016a): First investigations for a synthetic covariance matrix for monitoring by terrestrial laser scanning. 3rd Joint International Symposium on Deformation Monitoring, March 30–April 1, 2016, Vienna, Austria.

Kauker, S.; Schwieger, V. (2016b): A Synthetic Covariance Matrix for Monitoring by Terrestrial Laser Scanning. In: Journal of Applied Geodesy (in preparation).

Kermarrec, G.; Schön, S. (2014): On the Mátern covariance family: a proposal for modeling temporal correlations based on turbulence theory. In: Journal of Geodesy, 88(2014), 1061–1079. doi:10.1007/s00190-014-0743-7.

Koch, K. R. (2008): Determining uncertainties of correlated measurements by Monte-Carlo simulations applied to laserscanning. In: Journal of Applied Geodesy, 2(2008), 139–147.

Koch, K. R.; Kuhlmann, H.; Schuh, W. D. (2010): Approximating covariance matrices estimated in multivariate models by estimating auto- and cross-covariances. In: Journal of Geodesy, 84(2010), 383–397.

Kutterer, H.; Alkhatib, H.; Paffenholz, J.-A.; Vennegeerts, H. (2010): Monte-Carlo Simulation of Profile Scans from Kinematic TLS. Proceedings of FIG Congress 2010, Facing the Challenges – Building the Capacity, April 11–16, 2010, Sydney, Australia.

Matthias, H. J. (1986): Bedeutung und Konstruktionen von Kovarianzen in der Messtechnik. In: Mitteilungen des Instituts für Geodäsie und Photogrammetrie der ETH Zürich, 41.

Niemeier, W. (2007): Ausgleichungsrechnung. Statistische Auswertemethoden. 2nd Ed., W. de Gruyter, Berlin/New York.

Pelzer, H. (1985): Grundlagen der mathematischen Statistik und Ausgleichungsrechnung. In: Pelzer, H. (Ed.), Geodätische Netze in Landes- und Ingenieurvermessung II. Wittwer, Stuttgart.

Schabenberger, O.; Gotway, C. (2005): Statistical Methods for Spatial Data Analysis. Chapman & Hall/CRC Press, Boca Raton.

Schön, S.; Brunner, F. K. (2008): Atmospheric turbulence theory applied to GPS carrier-phase data. In: Journal of Geodesy, 82(2008)1, 47–57. doi:10.1007/s00190-007-0156-y.

Schön, S.; Kermarrec, G. (2015): Turbulence Theory. In: Freeden, W.; Nashed, Z.; Sonar, T. (Eds.): Handbook of Geomathematics. 2. Ed. doi:10.1007/978-3-642-27793-1_77-3.

Schwieger, V. (1999): Ein Elementarfehlermodell für GPS-Überwachungsmessungen. Schriftenreihe der Fachrichtung Vermessungswesen der Universität Hannover, 231.

Schwieger, V. (2007): Determination of Synthetic Covariance Matrices – An Application to GPS Monitoring Measurements. Proceedings of 15th European Signal Processing Conference, September 3–7, 2007, Poznan, Poland.

Dipl.-Ing. Stephanie Kauker

UNIVERSITÄT STUTTGART
INSTITUT FÜR INGENIEURGEODÄSIE

Geschwister-Scholl-Straße 24D | 70174 Stuttgart
stephanie.kauker@ingeo.uni-stuttgart.de

Dr.-Ing. Christoph Holst

UNIVERSITÄT BONN
INSTITUT FÜR GEODÄSIE UND
GEOINFORMATION (IGG)

Nussallee 17 | 53115 Bonn
c.holst@igg.uni-bonn.de

Prof. Dr.-Ing. habil. Volker Schwieger

UNIVERSITÄT STUTTGART
INSTITUT FÜR INGENIEURGEODÄSIE

Geschwister-Scholl-Straße 24D | 70174 Stuttgart
volker.schwieger@ingeo.uni-stuttgart.de

Prof. Dr.-Ing. Heiner Kuhlmann

UNIVERSITÄT BONN
INSTITUT FÜR GEODÄSIE UND
GEOINFORMATION (IGG)

Nussallee 17 | 53115 Bonn
heiner.kuhlmann@uni-bonn.de

Prof. Dr.-Ing. Steffen Schön

LEIBNIZ UNIVERSITÄT HANNOVER
INSTITUT FÜR GEODÄSIE

Schneiderberg 50 | 30167 Hannover
schoen@ife.uni-hannover.de

Manuskript eingereicht: 08.04.2016 | Im Peer-Review-Verfahren begutachtet